Journal of
Materials Chemistry C

Accepted Manuscript

This article can be cited before page numbers have been issued, to do this please use: H. Han, R. Cui, Y. Jing, G. Lu, Y. Zheng, L. Zhou, J. Zuo and H. Zhang, *J. Mater. Chem. C*, 2017, DOI: 10.1039/C7TC02117H.

ROYAL SOCIETY OF CHEMISTRY

rsc.li/materials-c

View Article Online
DOI: 10.1039/C7TC02117H

J. Mater. Chem. C

RSC Publishing

PAPER

Cite this: DOI: 10.1039/x0xx00000x

Highly efficient orange-red electroluminescence of iridium complexes with good electron mobility

Hua-Bo Han[1,#], Rong-Zhen Cui[2,#], Yi-Ming Jing[1], Guang-Zhao Lu[1], You-Xuan Zheng[*,1], Liang Zhou[*,2], Jing-Lin Zuo[1], Hongjie Zhang[2]

Received 00th January 2017,
Accepted 00th January 2017

DOI: 10.1039/x0xx00000x

www.rsc.org/MaterialsC

Two iridium complexes with 1-(2,6-*bis*(trifluoromethyl)pyridin-4-yl)isoquinoline (**tfmpiq**) and 4-(2,6-*bis*(trifluoromethyl)pyridin-4-yl)quinazoline (**tfmpqz**) main ligands and tetraphenylimidodiphosphinate (tpip) ancilary ligand were applied in organic light-emitting diodes (OLEDs). The introducing of quinazoline has greatly influence on the nature of the complex. The quantum yield and the electron mobility of **Ir(tfmpqz)$_2$(tpip)** are much higher than that of **Ir(tfmpiq)$_2$(tpip)** (**Ir(tfmpiq)$_2$(tpip)**: Φ: 0.47, μ_e: 8.93-9.47 × 10^{-6} cm^2 $V^{-1}s^{-1}$ under the electric field from 1040 $(V\ cm^{-1})^{1/2}$ to 1300 $(V\ cm^{-1})^{1/2}$; **Ir(tfmpqz)$_2$(tpip)**: Φ: 0.98, μ_e: 6.44-7.20 × 10^{-6} cm^2 V^{-1} s^{-1} under the electric field from 1040 $(V\ cm^{-1})^{1/2}$ to 1300 $(V\ cm^{-1})^{1/2}$). Besides, the **Ir(tfmpqz)$_2$(tpip)** based device also displayed better performances than that using **Ir(tfmpiq)$_2$(tpip).** Furthermore, with an europium complex $Eu(DBM)_3phen$ (DBM = dibenzoylmethide; phen = 1,10-phenanthroline) as a sensitizer, the device based on **Ir(tfmpqz)$_2$(tpip)** with a double emissive layers structure of ITO / MoO_3 (3 nm) / TAPC (50 nm) / Ir(tfmpqz)$_2$(tpip) (5 wt%): TcTa (10 nm) / $Eu(DBM)_3phen$ (0.2 wt%): Ir(tfmpqz)$_2$(tpip) (5 wt%): 26DCzPPy (10 nm) / TmPyPB (50 nm) / LiF (1 nm) / Al (100 nm) displayed best performances with a maximum luminance of 129 466 cd m^{-2}, a maximum current efficiency and a maximum power efficiency of 62.96 cd A^{-1} and 53.43 lm W^{-1}, respectively, with low efficiency roll-off. The current efficiency still remains as high as 58.84 cd A^{-1} at the brightness of 1 000 cd m^{-2} and 53.27 cd A^{-1} at the brightness of 5 000 cd m^{-2}, respectively. These results suggest that the Ir(III) complexes with quinazoline units are potential orange-red phosphorescent materials for OLEDs.

Introduction

The phosphorescent iridium(III) complexes have been extensively studied in organic light-emitting diodes (OLEDs) because of their high quantum efficiency and the wide range of emission colors.[1] The strong spin-orbit coupling (SOC) can promote triplet to ground radiative transition by introducing the central heavy atom, which leads to a quite high phosphorescence quantum efficiency in unusual. Furthermore, the phosphorescence of Ir(III) complexes generates by the metal-to-ligand charge transfers (MLCT) and ligand-centered (LC) transition,[2] so that it is possible to control the excited state's energy level by adjusting ligands via the substituent effect.

Quite high efficiency has been obtained for green phosphorescent devices, while the highest efficiency that has been reported for red emitters based devices is still much lower. Red emission is a crucial monochromatic light and also a pivotal constituent for the development of full-color display.[3] While the design of efficient red-emitting materials is much harder compared to other colors, which is consistent with the law of energy gap.[4] Most of red emitters are subjected to the heavy concession on the color purity and device efficiency. Because the characteristic emission is in the spectral zone where eyes are insensitive, luminosity of red devices is lower. Moreover, the difference between the host with wide bandgap and the red-emitting guest with narrow bandgap is quite enormous in the level of the highest occupied molecular orbital (HOMO) and/or lowest unoccupied molecular orbital (LUMO). Therefore, the guest molecule should be used as a deep trap for the electron and hole in an emitting layer, leading to an enhancement of the driving voltage. In addition, for red dopants, the self-quenching and triplet-triplet annihilation are too serious to be ignored especially when the doping concentrations are high. Thus, from perspective of reality, solving the above issues via the design of materials or/and the optimization of device is inevitable.[5]

Since tris(1-phenylisoquinline)iridium(III) $Ir(piq)_3$ and *bis*(1-phenyl-isoquinoline)(acetylacetonato)iridium(III) $Ir(piq)_2(acac)$ have been synthesized as red PHOLEDs materials by Y.-J. Su et al. the first time,[6] many efficient red emitters and devices have been developed based on isoquinoline derivatives due to their high electron affinities.[7] R.-H. Liu and K.-T. Wong used bulky and halogen substituent to reduce the impact of self-quenching.[8] Wong et al. reported a range of red emitters combining 9-arylcarbazole and triphenylamine in complex $Ir(piq)_2(acac)$.[9] Wong and Chen groups have suppressed close packing among the molecules by increasing steric hindrance.[10] In addition, great efforts have been made based on 2-phenylquinoline (phq), 2,4-diphenylquinoline, pyridine derivatives and so on.[11]

It is well-known that the balance of the electron-hole injection and transport is necessary for high-efficiency OLEDs using the Ir(III) complexes because both the charge carrier balance deterioration and nonradioactive quenching processes increase will cause a serious efficiency roll-off. Since the majority of hole-transporting materials' hole mobility is much higher than the electron-transporting materials' electron mobility, the OLEDs

View Article Online
DOI: 10.1039/C7TC02117H

performances depend on electron transport's capability. Therefore, the use of ambipolar host materials is essential to gain phosphorescent OLEDs with low efficiency roll-off, as well as the synthesis of dopants with excellent electron mobility.[12]

From our previous work, we found that tetraphenylimidodiphosphinate (tpip) is a good ancillary ligand for Ir(III) complexes due to their four bulky aromatic groups, leading to an increase of the spatial separation from neighboring molecules to suppress TTA (triplet-triplet annihilation), TPA (triplet-polaron annihilation) effectively,[13] as well as the ability of Ph_2P=O to improve the ability of electron injection and transportation.[14] Moreover, the bulky CF_3 substituents can affect the molecular packing and the steric protection surrounding the metal would restrain the self-quenching impact, and the C-F bond with low vibrational frequency can reduce radiationless deactivation rate.[15] Besides that, nitrogen heterocycle would also enhance the electron affinity and the electron mobility of the Ir(III) complexes.

Therefore, aiming to get efficient devices by improving the electron mobility, both 2,6-*bis*-trifluoromethyl-pyridine and quinazoline were introduced to replace the widely used phenyl and piq units. The complexes **Ir(tfmpiq)$_2$(tpip)** (**tfmpiq** = 1-(2,6-*bis*(trifluoromethyl)pyridin-4-yl)isoquinoline) and **Ir(tfmpqz)$_2$(tpip)** (**tfmpqz** = 4-(2,6-*bis*(trifluoromethyl)pyridin-4-yl)quinazoline) displayed emissions peak at 591 and 588 nm, respectively. Besides, the devices with both complexes showed good performances, and the device based on **Ir(tfmpqz)$_2$(tpip)** displayed better performances than the device based on **Ir(tfmpiq)$_2$(tpip)** due to the higher photoluminescence (PL) efficiency and better electron mobility.

Furthermore, aiming to enhance the EL performances based on Ir**(tfmpqz)$_2$(tpip),** we employed an europium(III) complex Eu(DBM)$_3$phen (DBM = dibenzoylmethide; phen = 1,10-phenanthroline) with low-lying highest occupied molecular orbital (HOMO) and/or lowest unoccupied molecular orbital (LUMO) levels to sensitize the Ir(III) complex in an electron dominant light-emitting layer (EML). Consequently, the device displayed the best performances with a maximum current efficiency ($\eta_{c,max}$) of 62.96 cd A^{-1} with low efficiency roll-off. Because of the low doped concentration (0.2 wt%) of the Eu(III) complex, the cost of this type device for practical application is not increase greatly from the industrial and economical point of view.

Results and discussion

Preparation and X-ray crystallography

Scheme 1 shows the chemical structures and synthetic routes of ligands and Ir(III) complexes. The reaction of 2,6-*bis*(trifluoromethyl)-pyridine with LDA (lithium diisopropylamide) and B(OPr-*i*)$_3$ gave two crude aryl boronic acids. The corresponding two trifluoromethyl fluorinated bipyridine ligands (**tfmpiq** and **tfmpqz**) were synthesized using a Suzuki coupling reaction. The tetraphenylimidodiphosphinate acid (Htpip) and potassium salt (Ktpip) were prepared according to our previous publications. The iridium complexes were obtained in two steps with popular methods via Ir(III) chloro-bridged dimer. Purification of the mixture by silica gel chromatography provided crude products, which were further purified by vacuum sublimation. All the new compounds were fully characterized by ^{1}H NMR, the electrospray ionization mass spectra (ESI-MS) and elemental analyses.

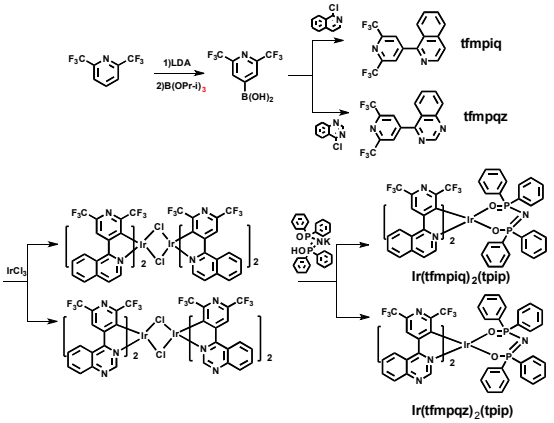

Scheme 1. Synthetic routes of ligands and the complexes.

Furthermore, The structures of **Ir(tfmpiq)$_2$(tpip)** and **Ir(tfmpqz)$_2$(tpip)** complexes were proved via the single crystals and their crystal diagrams are displayded in Fig. 1. The molecular parameters and atomic coordinates were showed in the Table S1, Table S2 (Supporting Information), respectively. From the structures diagram of crystals it can be found that the iridium atom is embraced by C, N and O atoms from **tfmpiq**/**tfmpqz** or tpip, with a twisted octahedral coordination geometry. For **Ir(tfmpiq)$_2$(tpip)** and **Ir(tfmpqz)$_2$(tpip)**, angles of [O-Ir-O] are 89.94(13)° - 90.64(12)°, and the angle of [C-Ir-N] is 80.06(14)° - 80.72(18)°. The lengths of Ir-C bonds range from 1.992(4) - 2.010(4) Å. The Ir-N bonds have the lengths of 2.024(4) - 2.038(3) Å. And the lengths of Ir-O bonds are longer a bits, which are 2.157(3) - 2.167(3) Å. These results are similar to the parameters of the cyclometalated Ir(III) complexes that have been reported.

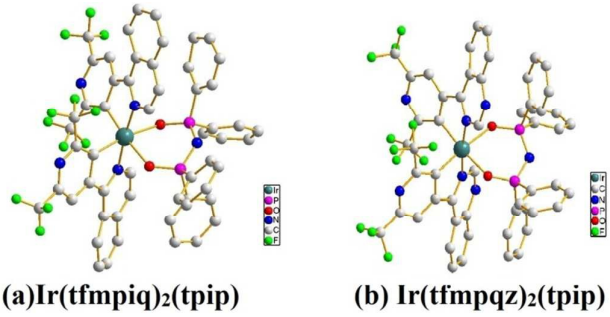

Fig. 1. The crystal diagrams of **Ir(tfmpiq)$_2$(tpip)** (CCDC No.1536092) and **Ir(tfmpqz)$_2$(tpip)** (CCDC No.1536093) shown at 30% probability level. The hydrogen atoms are omitted for clarity.

Thermal stability

The thermal stability of the materials is crucial for efficient OLEDs. If a complex can be applied in practical OLEDs, the melting point (T_m) and decomposition temperature (T_d) need to

View Article Online
DOI: 10.1039/C7TC02117H

be high enough to guarantee that the complex could be deposited onto the solid face without any decomposition on sublimation. The scanning calorimetry (DSC) and thermogravimetric analysis (TGA) curves of **Ir(tfmpiq)$_2$(tpip)** and **Ir(tfmpqz)$_2$(tpip)** are showed in Fig. S1. From the DSC crves it is can be seen that the melting points of **Ir(tfmpiq)$_2$(tpip)** and **Ir(tfmpqz)$_2$(tpip)** are 331 ^{o}C and 343 ^{o}C, respectively. It is can be figured out that there is no loss was observed below 340 ^{o}C in weight from the curves of TGA, and the decomposition temperature (5% loss of weight) is 357 ^{o}C for **Ir(tfmpiq)$_2$(tpip)** and 354 °C for **Ir(tfmpqz)$_2$(tpip)**, respectively, suggesting that both complexes have the potential for use in OLEDs. In general, the efficiency of vacuum-deposited OLEDs is much higher than that of solution-processed devices.

Electrochemical properties and theoretical calculation

The frontier molecular orbitals (FMOs), especially the HOMO and LUMO, are pretty crucial to the design of device structure. Therefore, aiming to measure energy levels of the HOMO/LUMO, the electrochemistry measurements by cyclic voltammetry (CV) were adopted with ferrocene as the internal standard in CH_3CN (Fig. S2). The HOMO level was obtained via the oxidation potential and then the LUMO level was calculated by the HOMO and the band gap observed from UV-vis absorption spectra. During the progress of anodic oxidation, an obvious oxide peak can be observed for all complexes with the oxidation potential in 1.31-1.51 V, which can be ascribed to the metal-centered Ir(III)/Ir(IV) oxide couple, consistent with the cyclometallated Ir(III) system reported.[16] **Ir(tfmpiq)$_2$(tpip)** exhibits a lower oxidation potential (1.31 V) and HOMO/LUMO energy levels are -5.94/-3.87 eV. The oxidation potential of **Ir(tfmpiq)$_2$(tpip)** increases to 1.51 V and the HOMO/LUMO energy levels are -6.25/-4.14 eV.

Furthermore, it can be observed from the theoretical calculation that nearly all LUMOs are on **tfmpiq**/**tfmpqz** ligands (94.73-95.11%) and rarely situated on iridium atom (2.98-3.378%) and tpip ancillary ligand (1.52-2.28%). While HOMOs are situated on **tfmpiq** ligands (46.07%), *d* orbitals on iridium atom (48.14%) and tpip ancillary ligand (5.79%) for **Ir(tfmpiq)$_2$(tpip)**. For **Ir(tfmpqz)$_2$(tpip)**, HOMOs are situated on **tfmpqz** ligands (36.88%) and *d* orbitals of iridium atom (53.77%) and tpip ancillary ligand (9.35%).[17] The introducing of quinazoline does influence the electron distributions of the complexes, resulting the decrease of the HOMO and LUMO level, which lead to the nature differences of **Ir(tfmpiq)$_2$(tpip)** and **Ir(tfmpqz)$_2$(tpip)**. What's more, the decrease of the LUMO level is beneficial to trap the electron and broaden the recombination zone, leading to the improvement of the EL performances partly.

Photophysical property

The UV-vis absorption and photoluminescence spectra of the two complexes **Ir(tfmpiq)$_2$(tpip)** and **Ir(tfmpqz)$_2$(tpip)** in CH_2Cl_2 (5×10^{-5} M) are shown in Fig. 2. The broad and intensive absorption bands below 320 nm are due to the spin-allowed intraligand ^{1}LC (π-π*) transition of **tfmpiq**/**tfmpqz** and tpip ligands. The weak absorption lasting to 520 nm should be attributed to the metal-ligand charge transfer band (MLCT), and/or broad LC absorptions. The strongest emissions peak at 591 and 588 nm in CH_2Cl_2, produced by the electronic transition between the lowest triplet excited state and the ground state, which makes **Ir(tfmpiq)$_2$(tpip)** and **Ir(tfmpqz)$_2$(tpip)** orange-red phosphors. The emissions in the scope of lower energy around 637 nm may generate by the overlapping vibrational satellites.[18] Furthermore, the complexes show much high quantum efficiency as 0.47 and 0.98 for **Ir(tfmpiq)$_2$(tpip)** and **Ir(tfmpqz)$_2$(tpip)**, respectively. The differences of the absorption and emission profiles between **Ir(tfmpiq)$_2$(tpip)** and **Ir(tfmpqz)$_2$(tpip)** suggest that the introduction of quinazoline does have an obvious effect, and it can increase the quantum efficiency greatly. Furthermore, the phosphorescence lifetime (τ) is the crucial factor that determines the rate of triplet-triplet annihilation in OLEDs. Longer τ values usually cause greater triplet-triplet annihilation. The lifetimes of the the complexes are in the range of microseconds (2.70 and 2.44 μs in CH_2Cl_2 solution respectively) at room temperature (Fig. S3 and Table 1) and are indicative of the phosphorescent origin for the excited states in each case.

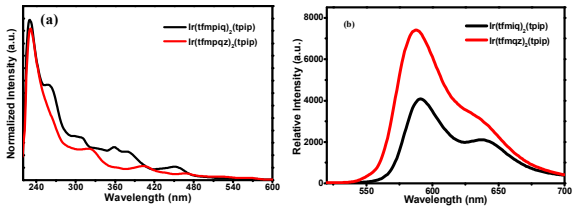

Fig. 2. (a) UV-vis absorption and (b) emission spectra of **Ir(tfmpiq)$_2$(tpip)** and **Ir(tfmpqz)$_2$(tpip)** complexes in degassed CH_2Cl_2 solutions (5.0×10^{-5} mol L^{-1}) at room temperature.

Table 1. Physical properties of **Ir(tfmpiq)$_2$(tpip)** and **Ir(tfmpqz)$_2$(tpip)**.

Complex	T_m/T_d [a] (°C)	λ_{abs} [b] (nm)	λ_{em} [c] (nm)	Φ [d]	τ [e] (μs)	HOMO/LUMO [f] (eV)
Ir(tfmpiq)$_2$(tpip)	331/357	358/377/451	591	0.47	2.70	-5.94/-3.87
Ir(tfmpqz)$_2$(tpip)	343/354	319/403/468	588	0.98	2.44	-6.25/-4.14

[a] T_m: melting temperature, T_d: decomposition temperature; [b], [c], [e] Measured in degassed CH_2Cl_2 solution at a concentration of 5×10^{-5} mol·L^{-1} at room temperature; [d] Measured in degassed CH_2Cl_2 solution at a concentration of 5×10^{-5} mol·L^{-1} at room temperature emission relative to $Ir(ppy)_3$ (Φ = 0.4); [f] From the onset of oxidation potentials of the cyclovoltammetry (CV) diagram using ferrocene as the internal standard and the optical band gap from the absorption spectra in degassed solution (CH_3CN).

View Article Online
DOI: 10.1039/C7TC02117H

Electron mobility

According to our previous studies, an excellent electron mobility of emitters could benefit electron transport and improve the device efficiency.[20] To determine the two complexes' electron mobility, the transient electroluminescence (TEL) measurement was carried out via the devices with a structure of ITO (indium-tin-oxide) / TAPC (1,1-*bis*[4-[N,N-di(p-tolyl)amino] phenyl]cyclohexane, 50 nm) / Ir complexes (60 nm)/ Li (1 nm) / Al (100 nm).[21] The Ir complexes act as not only the emissive layer (EML) but also electron-transport layer. The experimental results (Fig. 3) indicated that the electron mobility values of **Ir(tfmpiq)$_2$(tpip)** and **Ir(tfmpqz)$_2$(tpip)** are 6.44-7.20 × 10^{-6} cm^2 V^{-1} s^{-1} and 8.93-9.47 × 10^{-6} cm^2 $V^{-1}s^{-1}$, respectively, under the electric field from 1040 $(V\ cm^{-1})^{1/2}$ to 1300 $(V\ cm^{-1})^{1/2}$, higher than that of Alq_3 (aluminum 8-hydroxyquinolinate, 4.74-4.86 ×10-6 cm^2 V^{-1} s^{-1}).[22] Furthermore, the electron mobility of the classic red emit $Ir(piq)_2(acac)$ was also measured under the same conditions and the values are 5.62-5.92 × 10^{-6} cm^2 V^{-1} s^{-1} under the electric field from 1040 $(V\ cm^{-1})^{1/2}$ to 1300 $(V\ cm^{-1})^{1/2}$, lower than that of **Ir(tfmpiq)$_2$(tpip)** and **Ir(tfmpqz)$_2$(tpip)** (Fig. S4.)**.** Additionally, the electron mobility of **Ir(tfmpqz)$_2$(tpip)** is better than that of **Ir(tfmpiq)$_2$(tpip)** suggesting that quinzoline has the strong impact on the enhancement of the electron flow. The result is exactly fitting our design intent to improve the electron transport ability of the emitter. The good electron transport ability of **Ir(tfmpiq)$_2$(tpip)** and **Ir(tfmpqz)$_2$(tpip)** will reinforce the recombination chance of electrons and holes, so that their devices may have good performances, especially for that using **Ir(tfmpqz)$_2$(tpip)**.

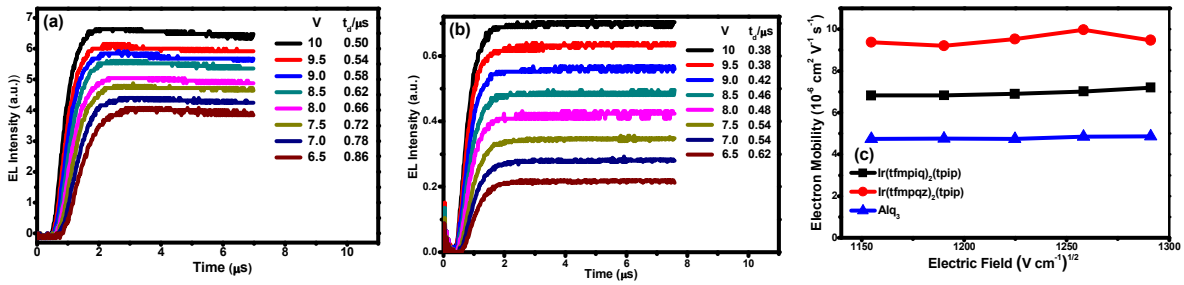

Fig. 3. (a), (b) the transient EL signals for the device structure of ITO/TAPC (50nm)/Ir complexes (60nm) under different applied fields of **Ir(tfmpiq)$_2$(tpip)** and **Ir(tfmpqz)$_2$(tpip)**; (c) electric field dependence of charge electron mobility in the thin films of **Ir(tfmpiq)$_2$(tpip)** and **Ir(tfmpqz)$_2$(tpip)** and Alq_3.

OLEDs performance

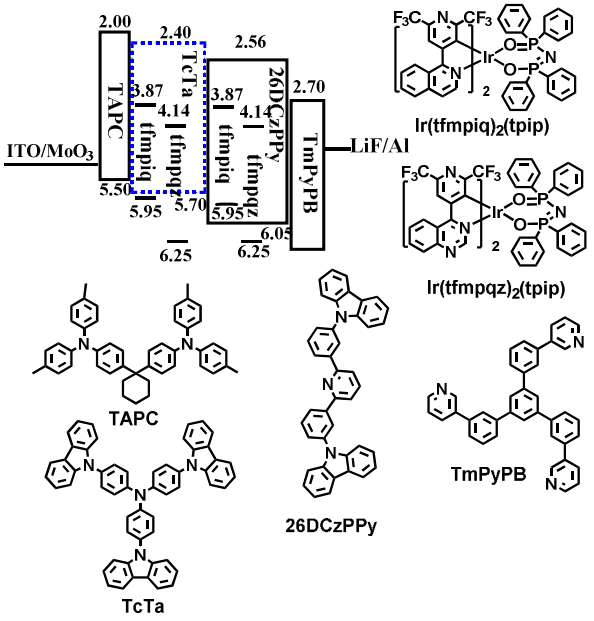

Fig. 4. Energy level diagram of HOMO and LUMO levels of materials used in this work and their molecular structures.

To confirm our assumption, we researched the single emitting layer (EML) devices G1 and G2 using **Ir(tfmpiq)$_2$(tpip)** and **Ir(tfmpqz)$_2$(tpip)** emitters, respectively, with a structure of ITO / MoO_3 (molybdenum oxide, 3 nm) / TAPC (50 nm) / Ir complex (x wt%): TcTa (4,4',4"-tris(carbazole-9-yl)triphenylamine, 10 nm) / TmPyPB (1,3,5-tri(m-pyrid-3-yl-phenyl)benzene, 50 nm) / LiF (1 nm) / Al (100 nm) (Fig. 4). MoO_3 and LiF served as hole- and electron-injecting interface modified materials, respectively. TAPC owning high hole mobility (1 × 10^{-2} cm^2 V^{-1} s^{-1}) and high-lying LUMO level (-2.0 eV) was used as hole transport/electron block layer (HTL/EBL), while TmPyPB with high electron mobility (1 × 10^{-3} cm^2 V^{-1} s^{-1}) and low-lying HOMO level (-6.7 eV) was used as electron transport/hole block layer (ETL/HBL). Ambipolar material 26DCzPPy was chosen as the host because its' nearly equal electron mobility (μ_e) and hole mobility (μ_h) values (1-8 × 10^{-5} cm^2 V^{-1} s^{-1} at an electric field between 6.0 × 10^5 and 1.0 × 10^6 V cm^{-1}), which benefits the electron-hole balance in the EML.[23-25] The optimal device performances are achieved at doping level of 6% and 5% for **Ir(tfmpiq)$_2$(tpip)** and **Ir(tfmpqz)$_2$(tpip)**, respectively.

The EL spectra, luminance-voltage-current density (*L-V-J*) curves, current efficiency-luminance (η_c-*L*) curves, power efficiency-luminance (η_p-*L*) curves for G1 and G2 are shown in Fig. S5, and the crucial EL data are shown in Table 2. The peaks of EL emission are 589 and 579 nm for G1 and G2, respectively, and the emission spectra are almost invariant of the current density (Fig. S6(a) and Fig. S6(b)) and there is no dependence on concentration. From the Fig.5(a), it is can be seen that the EL spectra are almost identical to the PL spectra of the complexes, suggesting that the devices' EL emissions come from the triplet excited states of the phosphors. Apart from the characteristic

View Article Online
DOI: 10.1039/C7TC02117H

emission of Ir complexes, these devices displayed weak emission range from 350 nm to 500 nm, which originate from the host 26DCzPPy attributed to the accumulation of holes and electrons within the EML and few holes/electrons would recombine on 26DCzPPy molecules. And the Commission Internationale de 1'Eclairage (CIE) color coordinates of G1 and G2 are (0.575, 0.414) and (0.532, 0.456), respectively.

For the device G1, a maximum current efficiency ($\eta_{c,max}$) of 20.13 cd A^{-1} (3.7 V) with a maximum external quantum efficiency (EQE_{max}) of 8.2%, a maximum power efficiency ($\eta_{p,max}$) of 19.32 lm W^{-1} (3.5 V) and a maximum luminance (L_{max}) of 45 902 cd m^{-2} were obtained. G2 exhibits much better performances with a L_{max} of 101 994 cd m^{-2} at 10.0 V, a $\eta_{c,max}$ of 52.68 cd A^{-1}, an EQE_{max} of 16.6%, and a $\eta_{p,max}$ of 42.87 lm W^{-1}. Moreover, G2 can remain high efficiency even at relatively high luminance and the EL efficiency roll-off is rather low. For instance, the current efficiency for the device G2 still keeps as high as 46.00 cd A^{-1} at the brightness of 1 000 cd m^{-2}. The higher PL efficiency (0.98) and better electron mobility (8.93-9.47 × 10^{-6} cm^2 $V^{-1}s^{-1}$ under the electric field from 1040 (V cm^{-1})$^{1/2}$ to 1300 (V cm^{-1})$^{1/2}$) of **Ir(tfmpqz)$_2$(tpip)** than that of **Ir(tfmpiq)$_2$(tpip)** would increase the device performances greatly.

Generally, the double-EMLs device could achieve better performances than the single-EMLs device because a better balance of carries and a wider recombination zone within EMLs could be realized by the double-EMLs device.[26] Thus, we researched the double-EML devices G3 and G4 using **Ir(tfmpiq)$_2$(tpip)** and **Ir(tfmpqz)$_2$(tpip)** emitters, respectively, with a structure of ITO / MoO_3 (3 nm) / TAPC (50 nm) / Ir complex (x wt%): TcTa (10 nm) / Ir complex (x wt%): 26DCzPPy (2,6-*bis*(3-(carbazol-9-yl)phenyl)pyridine, 10 nm) / TmPyPB (50 nm) / LiF (1 nm) / Al (100 nm). The optimal device performances are achieved at doping level of 6% and 5% for **Ir(tfmpiq)$_2$(tpip)** and **Ir(tfmpqz)$_2$(tpip)**, respectively.

The EL spectra, luminance-voltage-current density (*L-V-J*) curves, current efficiency-luminance (η_c-*L*) curves, power efficiency-luminance (η_p-*L*) curves for G3 and G4 are shown in Fig. 5, and the crucial EL data are shown in Table 2. The peaks of EL emission are 588 and 580 nm for G3 and G4, respectively, and the emission spectra are almost invariant of the current density (Fig. S6(c) and Fig. S6(d)) and there is no dependence on concentration. The CIE color coordinates of G3 and G4 are (0.579, 0.412) and (0.535, 0.453), respectively. From the Fig. 5(a), it is can be seen that the EL spectra are almost identical to the PL spectra of the complexes, and the weak emissions in the range of 350-500 nm were observed in the EL spectra of double-EML devices caused by the emission of TcTa peaked at 385 nm.

Compared with the single-EML devices, bot double-EML devices displayed better EL performances and lower efficiency roll-off. For the device G3, a $\eta_{c,max}$ of 22.39 cd A^{-1} (3.9 V) with an EQE_{max} of 10.3%, a $\eta_{p,max}$ of 18.75 lm W^{-1} (3.7 V) and a L_{max} of 54 426 cd m^{-2} were obtained. G4 exhibited much better performances with a L_{max} of 125 572 cd m^{-2} (9.6 V), a $\eta_{c,max}$ of 57.19 cd A^{-1}, an EQE_{max} of 18.7%, and a $\eta_{p,max}$ of 42.76 lm W^{-1}. Moreover, G4 can remain high efficiency even at relatively high luminance and the EL efficiency roll-off is rather low. For instance, the current efficiency for the device G4 still keeps as high as 54.19 cd A^{-1} at the brightness of 1 000 cd m^{-2} and 48.17 cd A^{-1} at the brightness of 5 000 cd m^{-2}, respectively, suggesting that the complex is a promising material in OLEDs.

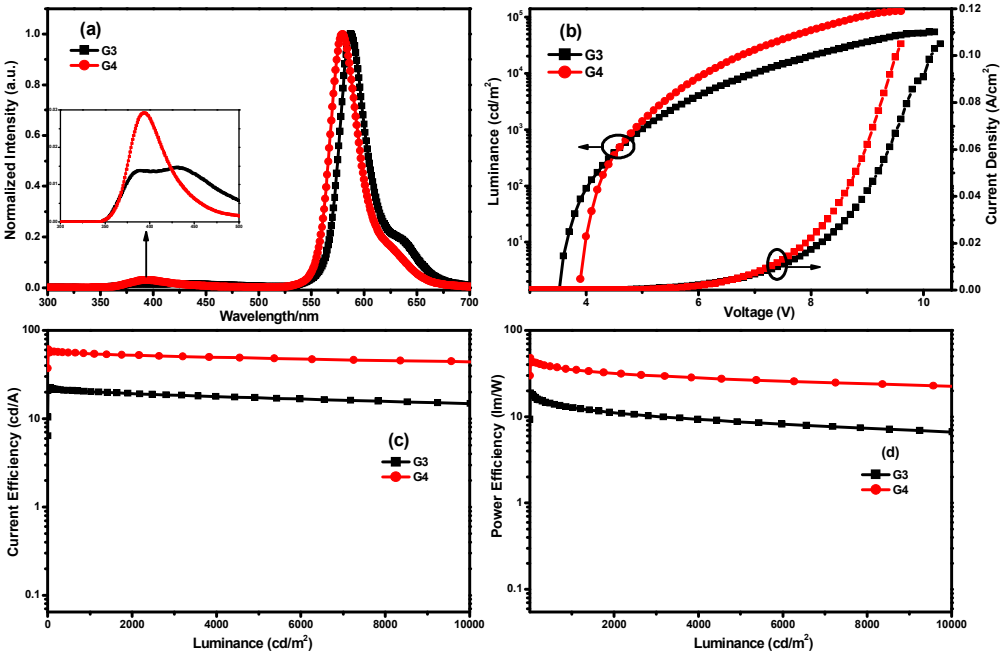

Fig. 5. Characteristics of double-EML devices G3 and G4: (a) electroluminescence spectra (100 mA); (b) luminance – voltage – current density (*L* – *V* – *J*) curves; (c) current efficiency – luminance (η_c – *L*) curves; (d) power efficiency – luminance (η_p – *L*) curves.

View Article Online
DOI: 10.1039/C7TC02117H

Because **Ir(tfmpqz)$_2$(tpip)** based device showed high efficiency, further work was done to increase its performances. A wide band gap trivalent europium complex Eu(DBM)$_3$phen (DBM = dibenzoylmethide, phen = 1,10-phenanthroline) was selected as a sensitizer codoped into the electron dominant EML of the double-EMLs devices because that Eu(DBM)$_3$phen can function as electron trappers due to its low-lying energy levels, which are helpful in balancing holes and electrons and in broadening recombination zone. Furthermore, the matched triplet energy of Eu(DBM)$_3$phen is instrumental in facilitating energy transfer from host to emitter.[27] The device G5 with a structure of ITO / MoO_3 (3 nm) / TAPC (50 nm) / Ir(tfmpqz)$_2$(tpip) (5%): TcTa (10 nm) / Eu(DBM)$_3$phen (y%): Ir(tfmpqz)$_2$(tpip) (5%): 26DCzPPy (10 nm) / TmPyPB (50 nm) / LiF (1 nm) / Al (100 nm) displayed better performances. The EL spectrum, *L*-*V*-*J*, η_c-*L* and η_p-*L* curves for G5 are show in Fig. 6, and the key EL data are also showed in Table 2. The device performances are the best at y = 0.2 wt% with a maximum luminance of 129 466 cd m^{-2} (10 V), a maximum current efficiency of 62.96 cd A^{-1}, a maximum external quantum efficiency of 20.2%, and a maximum power efficiency of 53.43 lm W^{-1} (3.7 V). In addition, the current efficiency for the device G5 still remain as high as 58.84 cd A^{-1} at the brightness of 1 000 cd m^{-2} and 53.27 cd A^{-1} at the brightness of 5 000 cd m^{-2}, respectively.

From the device performances, it is can be concluded that the introduction of 2,6-*bis*-trifluoromethyl-pyridine and quinazoline has definitely improved the electron mobility of the iridium complexes. As a result, the recombination chance of electrons and holes has been strengthened, which is beneficial to the improvement of OLEDs' performances. The devices structure of double EMLs is also useful for the better device efficiency due to the broad exciton formation zone. Furthermore, the efficiency based on **Ir(tfmpqz)$_2$(tpip)** has been risen greatly thanks to the sensitizer Eu(DBM)$_3$phen.

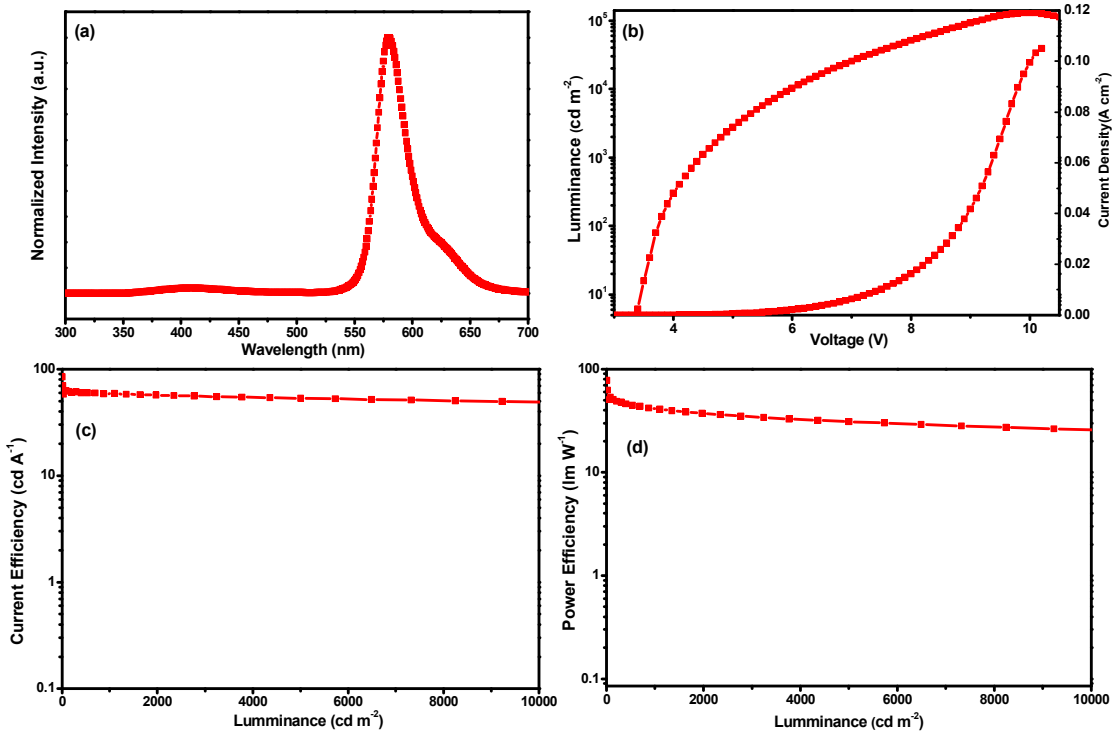

Fig. 6. Characteristics of the device G5: (a) electroluminescence spectra (100 mA); (b) luminance – voltage – current density (*L* – *V*– *J*) curves; (c) current efficiency – luminance (η_c – *L*) curves; (d) power efficiency – luminance (η_p – *L*) curves.

Table 2. EL performances of G1 – G5.

device	$V_{turn\text{-}on}$ [a] (V)	L_{max} [b] (cd m^{-2})	$\eta_{c,max}$ [c] (cd A^{-1})	$\eta_{c,L1000}$ [d] (cd A^{-1})	EQE_{max} [f] (%)	$\eta_{p,max}$ [g] (lm W^{-1})	*CIE(x,y)*
G1	3.2	45902	20.13	19.32	8.2	16.61	0.575,0.414
G2	3.6	101994	52.68	46.00	16.6	42.87	0.532,0.456
G3	3.5	54426	22.39	17.27	10.3	18.03	0.579,0.412
G4	3.9	125572	57.19	54.19	18.7	42.76	0.535,0.453
G5	3.4	129466	62.96	58.84	20.2	53.43	0.545,0.450

[a] $V_{turn\text{-}on}$: turn-on voltage recorded at a luminance of 1 cd m^{-2}. [b] L_{max}: maximum luminance. [c] $\eta_{c,max}$: maximum current efficiency. [d] $\eta_{c,L5000}$: current efficiency at 1 000 cd m^{-2}. [e] $\eta_{c,L10000}$: current efficiency at 10 000 cd m^{-2}. [f] EQE_{max}: maximum external quantum efficiency. [g] $\eta_{p,max}$: maximum power efficiency.

View Article Online
DOI: 10.1039/C7TC02117H

Conclusions

In conclusion, we have prepared two *bis*-cyclometalatted iridium complexes **Ir(tfmpiq)$_2$(tpip)** and **Ir(tfmpqz)$_2$(tpip)** with 1-(2,6-*bis*(trifluoromethyl)pyridin-4-yl)isoquinoline (**tfmpiq**) and 4-(2,6-*bis*(trifluoromethyl)pyridin-4-yl)quinazoline (**tfmpqz**) as the main ligands and tetraphenylimidodiphosphinate (tpip) as the ancilary ligand. Both complexes emit orange-red phosphorescence with high quantum efficiency and good electron mobility, **Ir(tfmpqz)$_2$(tpip)** especially. Through the comparison with the device using **Ir(tfmpiq)$_2$(tpip)**, the device using **Ir(tfmpqz)$_2$(tpip)** displays better EL performances and lower efficiency roll-off. Furthermore the device based on **Ir(tfmpqz)$_2$(tpip)** with Eu(DBM)$_3$phen as sensitizer shows better performances with a L_{max} of 129 466 cd m^{-2}, a $\eta_{c,max}$ of 62.96 cd A^{-1}, an EQE_{max} of 20.2% and a $\eta_{p,max}$ of 53.43 lm W^{-1}, respectively. The results suggest that the Ir(III) complexes with quinazoline units are potential orange-red phosphorescent materials for OLEDs.

Experimental section

General information

^{1}H NMR spectra were measured on a Bruker AM 500 spectrometer. Electrospray ionization mass spectra (ESI-MS) were obtained with ESI-MS (LCQ Fleet, Thermo Fisher Scientific). Elemental analyses for C, H and N were performed on an Elementar Vario MICRO analyzer. TG-DSC measurements were carried out on a DSC 823e analyzer (METTLER). UV-vis absorption and photoluminescence spectra were measured on a Shimadzu UV-3100 and a Hitachi F-4600 spectrophotometer at room temperature, respectively. Cyclic voltammetry measurements were conducted on a MPI-A multifunctional electrochemical and chemiluminescent system at room temperature using Fc^+/Fc as the internal standard and scan rate of 0.05 V s^{-1}.

X-ray crystallography

X-ray crystallographic measurements of the single crystals were carried out on a Bruker SMART CCD diffractometer (Bruker Daltonic Inc.) using monochromated Mo Kα radiation (λ = 0.71073 Å) at room temperature. Cell parameters were retrieved using SMART software and refined using *SAINT* [28] program in order to reduce the highly redundant data sets. Data were collected using a narrow-frame method with scan width of 0.30° in ω and an exposure time of 5 s per frame. Absorption corrections were applied using *SADABS* [29] supplied by Bruker. The structures were solved by Patterson methods and refined by full-matrix least-squares on F^2 using the program *SHELXS-2014*.[30] The positions of metal atoms and their first coordination spheres were located from direct-methods E-maps, other non-hydrogen atoms were found in alternating difference Fourier syntheses and least-squares refinement cycles and during the final cycles refined anisotropically. Hydrogen atoms were placed in calculated position and refined as riding atoms with a uniform value of U_{iso}.

OLEDs fabrication and measurement

All OLEDs were fabricated on the pre-patterned ITO-coated glass substrate with a sheet resistance of 15 Ω sq^{-1}. The deposition rate for organic compounds is 1-2 Å s^{-1}. The phosphor and host were co-evaporated from two separate sources. The cathode consisting of LiF/Al was deposited by evaporation of LiF with a deposition rate of 0.1 Å s^{-1} and then by evaporation of Al metal with a rate of 3 Å s^{-1}. The effective area of the emitting diode is 0.1 cm^2. The characteristics of the devices were measured with a computer controlled KEITHLEY 2400 source meter with a calibrated silicon diode in air without device encapsulation. On the basis of the uncorrected PL and EL spectra, the CIE coordinates were calculated using a test program of the spectra scan PR650 spectrophotometer.

Syntheses

All the reagents were used with commercial grade. The ligands and complexes were synthesized under nitrogen atmosphere and the synthetic routes were listed in Scheme 1.

General syntheses of ligands. A stirred solution of 2,6-*bis*-(trifluoromethyl)pyridine (0.22 g, 10mmol) in diethyl ether (20 mL) was cooled to -78 °C. LDA (lithium diisopropylamide, 6.0 mL, 10 mmol) was added over 20 min and stirred for 1 h, and then B(OPr-i)$_3$ (2.89mL,12.4mmol) was added. The mixture was warmed to room temperature and stirred for another 1 h. The pH was adjusted to 10 by the slow addition of 10% aqueous NaOH solution (20 mL). After 1 hour, the organic phase was acidified to pH = 4 by the dropwise addition of 3 N HCl. The extraction with ethyl acetate and evaporation of the organic phase gave the crude corresponding aryl boronic acids. 1-Chloroisoquinoline / 4-Chloroquinazoline (10 mmol) and *bis*(diphenylphosphion) ferrocene palladium (II) dichloromethane (0.3 mmol) and the boronic acids were added in 50mL THF. After 20 mL of aqueous 2 N K_2CO_3 was delivered, the reaction mixture was heated at 70 °C for 1 day under an nitrogen atmosphere. The mixture was poured into water and extracted with CH_2Cl_2 (10 mL × 3 times). Finally, silica column purification (PE:EA = 10:1) gave the 1-(2,6-*bis*(trifluoromethyl)pyridin-4-yl)isoquinoline and 4-(2,6-*bis*(trifluoromethyl)pyridin-4-yl)quinazoline.

1-(2,6-*Bis*(trifluoromethyl)pyridin-4-yl)isoquinoline. 40% yield. ^{1}H NMR (400 MHz, $CDCl_3$) δ 8.69 (d, J = 5.6 Hz, 1H), 8.26 (s, 2H), 8.00 (d, J = 8.3 Hz, 1H), 7.94 (dd, J = 8.5, 0.8 Hz, 1H), 7.81 (ddd, J = 8.2, 5.9, 1.2 Hz, 2H), 7.69 (ddd, J = 8.3, 6.9, 1.2Hz, 1H). MS(ESI) *m/z* calcd for $C_{16}H_8F_6N_2^+$: 352.06 $[M]^+$, found: 353.06 $[M+H]^+$.

4-(2,6-*Bis*(trifluoromethyl)pyridin-4-yl)quinazoline. 30% yield. ^{1}H NMR (400 MHz, $CDCl_3$) δ 9.49 (S, 1H),8.30 (S, 2H), 8.27 (d, J = 8.5 Hz, 1H),8.06 (ddd, J = 8.4, 6.9, 1.3Hz, 1H),7.96 (dd, J = 8.4, 0.6Hz, 1H),7.78 (ddd, J = 8.3, 7.0, 1.1 Hz, 1H). MS (ESI) *m/z* calcd. for $C_{15}H_7F_6N_3^+[M]^+$: 343.05, found 344.06$[M+H]^+$.

General syntheses of iridium complexes. A mixture of $IrCl_3$ (1 mmol) and tfmpiq or tfmpqz (2.5 mmol) in 2-ethoxyethanol and water (20 mL, 3:1, v/v) was refluxed for 24 h. After cooling, the solid precipitate was filtered to give the crude cyclometalated Ir(III) chloro-bridged dimer. Then, the slurry of crude

View Article Online
DOI: 10.1039/C7TC02117H

chloro-bridged dimer (0.2 mmol) and Ktpip (0.5 mmol) in 2-ethoxyethanol (20 mL) was refluxed for 24 h. The solvent was evaporated at low pressure and the mixture was poured into water and extracted with CH_2Cl_2 (10 mL × 3 times), and then chromatographed to give complexes $Ir(tfmpiq)_2(tpip)$ and $Ir(tfmpqz)_2(tpip)$, which were further purified by sublimation in vacuum.

$Ir(tfmpiq)_2(tpip)$. 46% yield. ^{1}H NMR (400 MHz, CDCl3) δ 8.89 (d, J = 6.6 Hz, 2H), 8.71 (d, J = 8.6 Hz, 2H), 8.51 (s, 2H), 7.85-7.59 (m, 10H), 7.44-7.30 (m, 6H), 6.93 (ddd, J =16.7,11.8,6.7 Hz, 6H), 6.67 (td, J = 7.4,1.3 Hz, 2H), 6.49 (td, J = 7.7,3.3 Hz, 4H). MS(ESI) *m/z* calcd for $C_{56}H_{34}F_{12}IrN_5O_2P_2$: 1291.16 $[M]^+$, found 1292.17 $[M+H]^+$. Anal. Calcd. For $C_{54}H_{32}F_{12}IrN_7O_2P_2$: C 52.05, H 2.65, N 5.42. Found: C 51.95, H 2.71, N 5.45.

$Ir(tfmpqz)_2(tpip)$. 27% yield. ^{1}H NMR (400 MHz, CDCl3) δ 9.69 (s, 2H), 8.61 (d, J = 11.7 Hz, 4H), 7.93 (d, J = 5.7 Hz, 4H), 7.88-7.82 (m, 2H), 7.71 (dd, J = 11.6, 7.3 Hz, 4H), 7.40 (d, J = 6.8 Hz, 6H), 6.96 (dd, J = 12.3, 7.5 Hz, 4H), 6.64 (t, J = 7.1 Hz, 2H), 6.53 (d, J = 6.9 Hz, 4H). MS(ESI) *m/z* calcd for $C_{54}H_{32}F_{12}IrN_7O_2P_2$: 1293.15 $[M]^+$, found 1294.17 $[M+H]^+$. Anal. Calcd. For $C_{54}H_{32}F_{12}IrN_7O_2P_2$: C 50.11, H 2.49, N 7.58. Found: C 49.94, H 2.97, N 7.71.

Acknowledgements

This work was supported by the Major State Basic Research Development Program (2013CB922101), the National Natural Science Foundation of China (21371093, 91433113, 21301095), the Natural Science Foundation of Jiangsu Province (BK20130054), Youth Innovation Promotion Association CAS (2013150), and Strategic Priority Research Program of the Chinese Academy of Sciences (XDB20000000).

Notes and references

[1] *State Key Laboratory of Coordination Chemistry, Jiangsu Key Laboratory of Advanced Organic Materials, Collaborative Innovation Center of Advanced Microstructures, School of Chemistry and Chemical Engineering, Nanjing University, Nanjing 210093, P. R. China, *e-mail: yxzheng@nju.edu.cn*

[2] *State Key Laboratory of Rare Earth Resource Utilization, Changchun Institute of Applied Chemistry, Chinese Academy of Sciences, Changchun 130022, P. R. China*

 # Han and Cui have the same contributions to this paper

†Electronic Supplementary Information (ESI) available. Parameters associated with the single crystal diffraction data, selected bond lengths and angles of **$Ir(tfmpiq)_2(tpip)$** and **$Ir(tfmpqz)_2(tpip)$**. The EL characteristics of single devices G1 and G2.

1 1 *(a)* S. Lamansky, P. Djurovich, D. Murphy, F. Abdel-Razzaq, H. E. Lee, C. Adachi, P. E. Burrow, S. R. Forrest and M. E. Thompson, *J. Am. Chem. Soc.*, 2001, **123**, 4304; *(b)* J. J. Kim, Y. You, Y. S. Park, J. J. Kim and S. Y. Park, *J. Mater. Chem.*, 2009, **19**, 8347; *(c)* Z. Q. Chen, Z. Q. Bian and C. H. Huang, *Adv. Mater.*, 2010, **22**, 1534; *(d)* S. M. Chen, G. P. Tan, W. Y. Wong and H. S. Kwok, *Adv. Funct. Mater.*, 2011, **21**, 3785; *(e)* J. M. Fernández-Hernández, C. H. Yang, J. I. Beltrán, V. Lemaur, F. Polo, R. Fröhlich, J. Cornil and L. D. Cola, *J. Am. Chem. Soc.*, 2011, **133**, 10543; *(f)* K. Y. Lu, H. H. Chou, C. H. Hsieh, Y. H. O. Yang, H. R. Tsai, H. Y. Tsai, L. C. Hsu, C. Y. Chen, I. C. Chen and C. H. Cheng, *Adv. Mater.*, 2011, **23**, 4933; *(g)* C.-H. Fan, P. Sun, T.-H. Su and C.-H. Cheng, *Adv. Mater.*, 2011, **23**, 2981; *(h)* S. Lee, S. O. Kim, H. Shin, H. J. Yun, K. Yang, S. K. Kwon, J. J. Kim and Y. H. Kim, J. Am. Chem. Soc., 2013, **135**, 14321; *(i)* X. L. Yang, N. Sun, J. S. Dang, Z. Huang, C. L. Yao, X. B. Xu, C. L. Ho, G. J. Zhou, D. G. Ma, X. Zhao and W. Y. Wong, *J. Mater. Chem. C*, 2013, **1**, 3317; *(j)* H. Sasabe, H. Nakanishi,Y. Watanabe,S. Yano, M. Hirasawa, Y.J. Pu and J. Kido, *Adv. Funct. Mater.*, 2013, **23**, 5550; *(k)* H.-H. Chou, Y.-K. Li, Y.-H. Chen, C.-C. Chang, C.-Y. Liao and C.-H. Cheng, *ACS Appl. Mater. Interfaces*, 2013, **5**, 6168; *(l)* V. K. Rai, M. Nishiura, M. Takimoto and Z. Hou, *J. Mater. Chem. C*, 2014, **2**, 5317; *(m)* H. Cao, H. Sun, Y. Yin, X. Wen, G. Shan, Z. Su, R. n. Zhong, W. Xie, P. Li and D. Zhu, *J. Mater. Chem. C*, 2014, **2**, 2150; *(n)* A.Graf, P. Liehm, C.Murawski, S. Hofmann, K. Leo and M. C. Gather, *J. Mater. Chem. C*, 2014, **2**, 10298; *(o)* X. Xu, X. Yang, J. Dang, G. Zhou, Y. Wu, H. Li and W.-Y. Wong, *Chem. Commun.*, 2014, **50**, 2473; *(p)* X. Yang, G. Zhou and W.-Y. Wong, *J. Mater. Chem. C*, 2014, **2**, 1760.

2 W. S. Jeon, T. J. Park, S. Y. Kim, R. Pode, J. Jang and J. H. Kwon, *Appl. Phys. Lett.*, 2008, **93**, 063303.

3 *(a)* A. Tsuboyama, H. Iwawaki, M. Furugori, T. Mukaide, J. Kamatani, S. Igawa, T. Moriyama, S. Miura, T. Takiguchi, S. Okada, M. Hoshino and K. Ueno, *J. Am. Chem. Soc.*, 2003, **125**, 12971; *(b)* S. Okada, K.Okinaka, H. Iwawaki, M. Furugori, M. Hashimoto, T. Mukaide, J. Kamatani, S. Igawa, A. Tsuboyama, T. Takiguchi and K. Ueno, *Dalton Trans.*, 2005, **9**, 1583; *(c)* G. Zhou, C. L. Ho, W. Y. Wong, Q. Wang, D. Ma, L. Wang, Z. Lin, T. B. Marder and A. Beeby, *Adv. Funct. Mater.*, 2008, **18**, 499; *(d)* J. C. Deaton, R. H. Young, J. R. Lenhard, M. Rajeswaran and S. Huo, *Inorg. Chem.*, 2010, **49**, 9151; *(e)* C. L. Ho, L. C. Chi, W. Y. Hung, W. J. Chen, Y. C. Lin, H. Wu, E. Mondai, G. J. Zhou, K. T. Wong and W. Y. Wong, *J. Mater. Chem. C*, 2012, **22**, 215; *(f)* C. L. Ho, B. Yao, B. Zhang, K. L. Wong, W. Y. Wong, Z. Xie, L. Wang and Z. Lin, *J. Organomet. Chem.*, 2013, **730**, 144; *(g)* G. M. Li, D. X. Zhu, T. Peng, Y. Liu, Y. Wang and M. R. Bryce, *Adv. Funct. Mater.*, 2014, **24**, 7420; *(h)* G. J. Li, J. Ecton, B. O'Brien and J. Li, *Org. Electron.*, 2014, **15**, 1862; *(i)* X. B. Xu, X. L. Yang, Y. Wu, G. J. Zhou, C. Wu and W. Y. Wong, *Chem. Asian J.*, 2015, **10**, 252; *(j)* X. L. Yang, X. B. Xu, J. S. Dang, G. J. Zhou, C. L. Ho and W. Y. Wong, *Inorg. Chem.*, 2016, **55**, 1720; *(k)* J. Lin, N. Y. Chau, J. L. Liao, W. Y. Wong, C. Y. Lu, Z. T. Sie, C. H. Chang, M. A. Fox, P. J. Low, G. H. Lee and Y. Chi, *Organometallics*, 2016, **35**, 1813; *(l)* X. J. Liu, B. Yao, Z. L. Zhang, X. F. Zhao, B. H. Zhang, W. Y. Wong, Y. X. Cheng and Z. Y. Xie, *J. Mater. Chem. C*, 2016, **4**, 5787.

4 *(a)* C.-T. Chen, *Chem. Mater.*, 2004, **16**, 4389; *(b)* S.D. Cummings and R. Eisenberg, *J. Am. Chem., Soc*., 1996, **118**, 1949.

5 C.-L. Ho, H. Li and W.-Y. Wong, *J. Organomet. Chem.*, 2014, **751**, 261.

6 *(a)* Y.-J. Su, H.-L. Huang, C.-L. Li, C.-H. Chien, Y.-T. Tao, P.-T. Chou, S. Datta and R.-S. Liu, *Adv. Mater.*, 2003, **15**, 884; *(b)* C.L. Li, Y.J. Su, Y.T. Tao, P.T. Chou, S. Datta and R.S. Liu, *Adv. Funct. Mater.*, 2005, **15**, 387.

7 *(a)* C. Adachi, M.A. Baldo, S.R. Forrest, S. Lamansky, M.E. Thompson, R.C. Kwong, *Appl. Phys. Lett.,* 2001, **78**, 1622; *(b)* P. Coppo, E.A. Plummer, L.D. Cola, *Chem. Commun.,* 2004, 1774.

View Article Online
DOI: 10.1039/C7TC02117H

8 H.-C. Ting, Y.-M. Chen, H.-W. You, W.-Y. Hung, S.-H. Lin, A. Chaskar, S.-H. Chou, Y. Chi, R.-H. Liu, K.-T. Wong, *J. Mater. Chem.*, 2012, **22**, 8399.

9 *(a)* G.-J. Zhou, W.-Y. Wong, B. Yao, Z. Xie, L. Wang, *Angew. Chem. Int. Ed*., 2007, **46**, 1149; *(b)* C.-L. Ho, W.-Y. Wong, Z.-Q. Gao. C.-H. Chen, K.-W. Cheah, B. Yao, Z. Xie, Q. Wang, L. Wang, X.-M. Yu, H.-S. Kwok, Z. Lin, *Adv. Funct. Mater.*, 2008, **18**, 319.

10 *(a)* G.-J. Zhou, W.-Y. Wong, B. Yai, Z. Xie, L. Wang, *J. Mater. Chem.,* 2008, **18**, 1799; (b) J.H. Yao, C. Zhen, K.P. Loh, Z.-K. Chen, *Tetrahedron*, 2008, **64**, 10814.

11 *(a)* D.H. Kim, N.S. Cho, H.-Y. Oh, J.H. Yang, W.S. Jeon, J.S. Park, M.C. Suh, J.H. Kwon, *Adv. Mater.*, 2011, **23**, 2721. *(b)* F.-I. Wu, H.-J. Su, C.-F. Shu, L. Luo, W.-G. Diau, C.-H. Cheng, J.-P. Duan, G.-H. Lee, *J. Mater. Chem.*, 2005, **15**, 1035. *(c)* S.-J. Lee, J.-S. Park, M. Song, I.A. Shin, Y.-I. Kim, J.W. Lee, J.-W. Kang, Y.-S. Gal, S. Kang, J.Y. Lee, S.-H. Jung, H.-S. Kim, M.-Y. Chae, S.-H. Jin, *Adv. Funct. Mater.*, 2009, **19**, 2205. *(d)* J. Ding, J. Lü, Y. Cheng, Z. Xie, L. Wang, X. Jing, F. Wang, *Adv. Funct. Mater.*, 2008, **18**, 2754. *(e)* J. Qiao, L. Duan, L. Tang, L. He, L. Wang, Y. Qiu, *J. Mater. Chem.*, 2009, **19**, 6573. *(f)* C.-L. Ho, L.-C. Chi, W.-Y. Hung, W.-J. Chen, Y.-C. Lin, H. Wu, E. Mondal, G.-J. Zhou, K.-T. Wong, W.-Y. Wong, *J. Mater. Chem.*, 2012, **22**, 215. *(g)* M. Tavasli, T.N. Moore, Y. Zheng, M.R. Bryce, M.A. Fox, G.C. Griffiths, V. Jankus, H.A. Al-Attar, A.P. Monkman, *J. Mater. Chem.*, 2012. **22**, 6419. *(h)* M. Zhu, Y. Li, S. Hu, C. Li, C. Yang, H. Wu, J. Qin, Y. Cao, *Chem. Commun*., 2012, **48**, 2695. *(i)* G.-J. Zhou, C.-L. Ho, W.-Y. Wong, Q. Wang, D. Ma, L. Wang, Z. Lin, T.B. Marder, A. Beeby, *Adv. Funct. Mater.*, 2008, **18**, 499. *(j)* G.-J. Zhou, Q. Wang, W.-Y. Wong, D. Ma, L. Wang, Z. Lin, *J. Mater. Chem*., 2009, **19**, 1872. *(k)* J. Li, R. Wang, R. Yang, W. Zhou, X. Wang, *J. Mater. Chem. C*, 2013, **1**, 4171. *(l)* B.X. Mi, P.F. Wang, Z.Q. Gao, C.S. Lee, S.T. lee, H.L. Hong, X.M. Chen, M.S. Wong, P.F. Xia, K.W. Cheah, C.H. Chen, W. Huang, *Adv. Mater.*, 2009, **21**, 339. *(m)* J.P. Duan, P.P. Sun, C.H. Cheng, *Adv. Mater.*, 2003, **15**, 224. *(n)* Q. Mei, L. Wang, Y. Guo, J. Weng, F. Yan, B. Tian, B. Tong, *J. Mater. Chem.*, 2012, **22**, 6878. *(h)* Y.-J. Pu, R.E. Harding, S.G. Stevenson, E.B. Namdas, C. Tedeschi, J.P.J. Markham, R.J. Rummings, P.L. Burn, I.D.W. Samuel, *J. Mater. Chem*., 2007, **17**, 4255. *(i)* H. Fukagawa, T. Shimizu, H. Hanashima, Y. Osada, M. Suzuki, H. Fujikake, *Adv. Mater.*, 2012, **24**, 5099. *(j)* E. Rossi, L. Murphy, P.L. Brothwood, A. Colombo, C. Dragonetti, D. Roberto, R. Ugo, M. Cocchi, J.A.G. Williams, J. Mater. Chem., 2011, **21**, 15501. *(k)* C. Borek, K. Hanson, P.I. Djurovich, M.E. Thompson, K. Aznavour, R. Bau, Y.R. sun, S.R. Forrest, J. Brooks, L. Michalski, J. Brown, *Angew. Chem. Int. Ed*., 2007, **46**, 1109. *(l)* T.-C. Lee, J.-Y. Hung, Y. Chi, Y.-M. Cheng, G.-H. Lee, P.-T. Chou, C.-C. Chen, C.- H. Chang, C.-C. Wu, *Adv. Funct. Mater.*, 2009, **19**, 2639.

12 *(a)* S. Heun and P. M. Borsenberger, *Chem. Phys.*, 1995, **200**, 245; *(b)* H. H. Fong, K. C. Lun and S. K. So, *Chem. Phys. Lett.*, 2002, **353**, 407.

13 *(a)* Y. C. Zhu, L. Zhou, H. Y. Li, Q. L. Xu, M. Y. Teng, Y. X. Zheng, J. L. Zuo, H. J. Zhang and X. Z. You, *Adv. Mater.*, 2011, **23**, 4041; *(b)* M. Y. Teng, S. Zhang, S. W. Jiang, X. Yang, C. Lin, Y. X. Zheng, L. Y. Wang, D. Wu, J. L. Zuo and X. Z. You, *Appl. Phys. Lett.*, 2012, **100**, 073303; *(c)* Q. L. Xu, C. C. Wang, T. Y. Li, M. Y. Teng, S. Zhang, Y. M. Jing, X. Yang, W. N. Li, C. Lin, Y. X. Zheng, J. L. Zuo and X. Z. You, *Inorg. Chem.*, 2013, **52**, 4916; *(d)* H. Y. Li, L. Zhou, M. Y. Teng, Q. L. Xu, C. Lin, Y. X. Zheng, J. L. Zuo, H. J. Zhang and X. Z. You, *J. Mater. Chem. C*, 2013, **1**, 560; *(e)* C. C. Wang, Y. M. Jing, T. Y. Li, Q. L. Xu, S. Zhang, W. N. Li, Y. X. Zheng, J. L. Zuo, X. Z. You and X. Q. Wang, *Eur. J. Inorg. Chem.*, 2013, 5683; *(f)* M. Y. Teng, S. Zhang, Y. M. Jin, T. Y. Li, X. Liu, Q. L. Xu, C. Lin, Y. X. Zheng, L. Wang and J. L. Zuo, *Dyes Pigm.*, 2014, **10**, 105; *(g)* Q. L. Xu, X. Liang, S. Zhang, Y. M. Jing, X. L., G. Z. Lu, Y. X. Zheng and J. L. Zuo, *J.Mater. Chem. C*,2015, **3**, 3694.

14 *(a)* H.-H. Chou and C.-H. Cheng, *Adv. Mater.*, 2010, **22**, 2468; (b) S. O. Jeon, S. E. Jang, H. S. Son and J. Y. Lee, *Adv. Mater.*, 2011, **23**, 1436.

15 Y. T. Tao, C. L. Yang and J. G. Qin, *Chem. Soc. Rev*., 2011, **40**, 2943.

16 S. Bettington, M. Tavasli, M. R. Bryce, A. Beeby, H. Al-Attar and A. P. Monkman, *Chem. – Eur. J.*, 2007, **13**, 1423.

17 *(a)* M. J. Frisch, G. W. Trucks, H. B. Schlegel, G. E. Scuseria, M. A. Robb, J. R. Cheeseman, G. Scalmani, V. Barone, B. Mennucci, G. A. Petersson, H. Nakatsuji, M. Caricato, X. Li, H. P. Hratchian, A. F. Izmaylov, J. Bloino, G. Zheng, J. L. Sonnenberg, M. Hada, M. Ehara, K. Toyota, R. Fukuda, J. Hasegawa, M. Ishida, T. Nakajima, Y. Honda, O. Kitao, H. Nakai, T. Vreven, J. A. Montgomery Jr., J. E. Peralta, F. Ogliaro, M. Bearpark, J. J. Heyd, E. Brothers, K. N. Kudin, V. N. Staroverov, R. Kobayashi, J. Normand, K. Raghavachari, A. Rendell, J. C. Burant, S. S. Iyengar, J. Tomasi, M. Cossi, N. Rega, J. M. Millam, M. Klene,J. E. Knox, J. B. Cross, V. Bakken, C. Adamo, J. Jaramillo, R. Gomperts, R. E. Stratmann, O. Yazyev, A. J. Austin, R. Cammi, C. Pomelli, J. W. Ochterski, R. L. Martin, K. Morokuma, V. G. Zakrzewski, G. A. Voth, P. Salvador, J. J. Dannenberg, S. Dapprich, A. D. Daniels, O. Farkas, J. B. Foresman, J. V. Ortiz, J. Cioslowski and D. J. Fox, *Gaussian 09, Revision A.01*, Gaussian, Inc., Wallingford, CT, 2009; *(b)* C. T. Lee, W. T. Yang and R. G. Parr, Phys. Rev. B: Condens. *Matter Mater. Phys.*, 1988, **37**, 785; *(c)* A. D. Becke, *J. Chem. Phys.*, 1993, **98**, 5648; *(d)* P. J. Hay, *J. Phys. Chem*., A, 2002, **106**, 1634; *(e)* S. Chiodo, N. Russo and E. Sicilia, *J. Chem. Phys.*, 2006, **125**, 104107; *(f)* M. Cossi, N. Rega, G. Scalmani and V. Barone, *J. Comput. Chem.*, 2003, **24**, 669.

18 A. F. Rausch, M. E. Thompson and H. Yersin, *Inorg. Chem.*, 2009, **48**, 1928.

19 *(a)* A. P. Wilde and R. J. Watts, *J. Phys. Chem.*, 1991, **95**, 622; *(b)* M. G. Colombo, T. C. Brunold, T. Riedener, H. U. Gudel, M. Fortsch and H. B. Burgi, *Inorg. Chem.*, 1994, **33**, 545.

20 *(a)* J. Kalinowski, W. Stampor, J. Mezyk, M. Cocchi, D. Virgili, V. Fattori and P. Di Marco, Phys. Rev. B: Condens. Matter Mater. Phys., 2002, **66**, 235321; *(b)* W. S. Jeon, T. J. Park, S. Y. Kim, R. Pode, J. Jang and J. H. Kwon, *Appl. Phys. Lett.*, 2008, **93**, 063303.

21 S. C. Tse, H. H. Fong and S. K. So, *J. Appl. Phys.*, 2003, **94**, 2033.

22 *(a)* H. Scher and E. W. Montroll, Phys. Rev. B: Solid State, 1975, **12**, 2455; *(b)* A. J. Pal, R. Osterbacka, K. M. Kallman and H. Stubb, *Appl. Phys. Lett.*, 1997, **71**, 228.

23 J. Lee, N. Chopra, S.-H. Eom, Y. Zheng, J. Xue, F. So and J. Shi, *Appl. Phys. Lett.*, 2008, **93**, 123306.

24 S.-J. Su, T. Chiba, T. Takeda and J. Kido, *Adv. Mater.*, 2008, **20**, 2125.

25 M. Ikai, S. Tokito, Y. Sakamoto, T. Suzuki and Y. Taga, *Appl. Phys. Lett.*, 2001, **79**, 156.

View Article Online
DOI: 10.1039/C7TC02117H

26 *(a)* X. Zhao, L. Zhou , Y. Jiang, R. Cui, Y. Li and H. Zhang, *Dyes and Pigments*, 2016, **130**, 148; *(b)* Y. Li, L. Zhou, Y. Jiang, R. Cui, X. Zhao, Y. Zheng, J. Zuo and H. Zhang, *RSC Adv.*, 2016, **6**, 63200; *(c)* Y. Li, L. Zhou, R. Cui, Y. Jiang, X. Zhao, W. Liu, Q. Zhu, Y. Cui and H. Zhang, *RSC Adv.*, 2016, **6**, 71282

27 L. Zhou, L. Li, Y. Jiang, R. Cui, Y. Li, X. Zhao and H. Zhang, *ACS Appl. Mater. Interfaces,*2015, 7, 16046.

28 *SAINT-Plus, version 6.02*, Bruker Analytical X-ray System, Madison, WI, 1999.

29 G. M. Sheldrick, *SADABS An empirical absorption correction program, Bruker Analytical X-ray Systems*, Madison, WI, 1996.

30 G. M. Sheldrick, *SHELXTL-2014*, Universität of Göttingen, Göttingen, Germany, 2014.

View Article Online
DOI: 10.1039/C7TC02117H

Graphical abstract

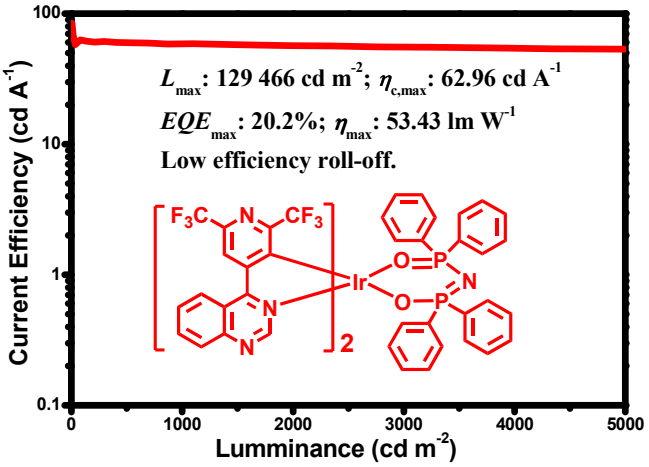

Two orange-red iridium complexes with high quantum yields and good electron mobility were applied in efficient OLEDs showing a maximum luminance of 129 466 cd m^{-2}, a maximum current efficiency and a maximum power efficiency of 62.96 cd A^{-1} and 53.43 lm W^{-1}, respectively, with low efficiency roll-off.